Influx and Efflux of Strigolactones Are Actively Regulated and Involve the Cell-Trafficking System

Accepted Manuscript

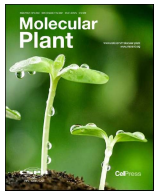

Influx and Efflux of Strigolactones are Actively Regulated and involve the Cell Trafficking System

Marcelo Fridlender, Beatrice Lace, Smadar Wininger, Anandamoy Dam, Puja Kumari, Eduard Belausov, Hanita Tsemach, Yoram Kapulnik, Cristina Prandi, Hinanit Koltai

PII: S1674-2052(15)00359-7
DOI: 10.1016/j.molp.2015.08.013
Reference: MOLP 178

To appear in: *MOLECULAR PLANT*
Accepted Date: 25 August 2015

Please cite this article as: **Fridlender M., Lace B., Wininger S., Dam A., Kumari P., Belausov E., Tsemach H., Kapulnik Y., Prandi C., and Koltai H.** (2015). Influx and Efflux of Strigolactones are Actively Regulated and involve the Cell Trafficking System. Mol. Plant. doi: 10.1016/j.molp.2015.08.013.

Influx and Efflux of Strigolactones are Actively Regulated and involve the Cell Trafficking System

Dear Editor,

Strigolactones (SLs) are plant hormones that regulate different aspects of plant development. In roots, SLs are involved in the regulation of lateral-root formation and they induce root-hair elongation. They are also exuded from plant roots and act as stimulators of parasitic and symbiotic (e.g., arbuscular mycorrhizae) interactions. SLs are perceived in plants by a specific reception system that consists of several interacting proteins (reviewed by Al-Babili and Bouwmeester, 2015).

A putative transporter of SLs was previously identified in petunia (*Petunia hybrida*): the ATP-binding cassette (ABC) protein designated PDR1. It was shown to have a key role in petunia in regulating the development of arbuscular mycorrhizae and axillary branches, by functioning as a cellular SL exporter (Kretzschmar et al., 2012). *pdr1* mutants were aberrant in symbiotic interactions and shoot phenotype, suggesting impaired SL allocation. In *Arabidopsis thaliana* overexpressing *Petunia axillaris* PDR1, tolerance to high concentrations of a synthetic SL was enhanced, suggesting increased export of SLs from the roots (Kretzschmar et al., 2012). However, only little is known about the movement of SLs, their precursors or their derivatives in general, and in *Arabidopsis* in particular.

Herein we present new evidence for SL distribution in the plant using fluorescent SL derivatives. Among the different fluorescently tagged SL-like compounds synthesized and tested in our laboratories, fluorescent BODIPY (BP)-tagged SL analogs have the desired bioactivity and spectroscopic properties (Prandi et al., 2014). Also, the SL analog EGO10 sharing the core structure with EGO10-BP, has been shown to act on the root to increase root-hair length (Cohen et al., 2013). Therefore, we synthesized EGO10-BP which is the SL analog EGO10 functionalized with green BP as the fluorophore (Supplemental Figure 1) by means of a 3 C linker. Four different BP derivatives differing in their structure were used: EGO10A-BP (pure enantiomer A), EGO10B-BP (pure enantiomer B), EGO10-mD-BP (SL analog EGO10-BP lacking the D-ring and the enol ether bridge) and naked-BP (fluorophore only). The EGO10-BP serie presents a simplified stereochemistry with respect to natural SLs as only a stereocenter is present at the C-2' position. Using CD spectra and chiral HPLC behaviour (not shown) EGO10A-BP was established to be the

enantiomer with natural SL structures (R configuration), conforming with canonical SLs structure.

Agar cubes containing fluorescent SLs (EGO10A-BP, EGO10B-BP,) or EGO10-mD-BP or naked-BP (at 10 µM concentration) were placed on Arabidopsis seedling roots (Supplemental Material and Methods and Supplemental Figure 2). Fluorescent signal was detected in the treated roots after 24 h and quantified (using IMAGEJ) in 9 segments of 100 µm each (Supplemental Figure 2), shoot-ward or root-ward from the agar cube placement.

The naked-BP treatment resulted in a very high signal in the root tissue (Supplemental Figure 3). The EGO10A-BP signal was significantly higher than that of EGO10B-BP or EGO10-mD-BP, both shoot-ward (Figure 1A) and root-ward (Supplemental Figure 3). Accordingly, EGO10A-BP was the most active analog for root-hair elongation in root segments above the agar cube compared to the other compounds tested (Figure 1B), similarly to the activity of EGO10A (Supplemental Figure 4). Also, placement of agar cube without any SL analog does not significantly change root-hair length in comparison to non-treated control (Supplemental Figure 4). Although shoot-ward signal was slightly higher than that of the root-ward, no significant differences between the two were detected (Supplemental Figure 3).

At the cellular level, EGO10A-BP signal was detected in the root epidermis and to a much lesser extent in root cortex and vascular tissues (Figure 1C). The naked-BP molecule signal was high in all root tissues: it was apparent mostly in the root cortex and vascular tissues, and to a relatively lesser extent in the root epidermis (Figure 1C). At the subcellular level, EGO10A-BP signal was detected in the cytoplasm, in vesicle-like bodies, in endosomal-like structures and in correspondence of nuclei, present to a smaller extent in the nucleus and labelling the nuclear envelope (Figure 1C; additional examples for images in Supplementary Fig 5). Since EGO10A-BP was biologically active (Figure 1B), it might be that the its relatively small extent in the nucleus was sufficient to acknowledge activity. The naked-BP molecule signal was distributed evenly across the cell cytoplasm (Figure 1C) and did not affect root hair elongation (Figure 1B).

Treatment with the fluorescent SLs and Antimycin A, an inhibitor of oxidative ATP production and of the electron flow in the mitochondrial respiratory chain (ATPi; 10 µM) in the agar cube resulted in a significant increase in signal in the first two segments of the root (shoot-ward) for EGO10A-BP but not for EGO10B-BP or

EGO10-mD-BP (Figure 1A). Only a minor significant difference between means of EGO10-mD-BP and EGO10-mD-BP + ATPi treatments were found in segment 7. A high signal for EGO10A-BP was also detected in uncut roots, in a region under the EGO10A-BP-containing agar cube (Supplemental Figure 6). Moreover, EGO10A-BP was only poorly transported shoot-ward in the EGO10A-BP + ATPi treatment in comparison to the EGO10A-BP-only treatment (slopes of -28.62 and -7.26 measured for the first three segments, respectively; Figure 1A, Supplemental Figure 7). It should be noted, however, that the ATPi effect may be restricted to the first few root segments, due to the restricted distribution of ATPi, and as a result, slops are similar between EGO10A-BP-only and EGO10A-BP + ATPi treatments in more distant root segments (Figure 1A). In addition, treatment with ATPi resulted with loss of subcellular compartmentalization (Supplemental Figure 6B).

Next, we examined the possible involvement of the cell trafficking system in SL cellular transport. We treated the roots with brefeldin A (BFA), which leads to the formation of BFA compartments due to its interference with trafficking of certain plasma membrane (PM) proteins in the cell via the trans-Golgi network/early endosome (TGN/EE) and to a retrograde transport of Golgi membrane protein into the endoplasmic reticulum (ER) (Robinson et al., 2008 and references within). Roots were exposed to the agar cubes containing the fluorescent compound for 24 h followed by BFA treatment for 2 h (100 µM) and staining with FM4-64. In this treatment, EGO10A-BP signal was detected in both the BFA and cytoplasmic compartments (Figure 1D). As expected, because trafficking is an active process, no BFA compartments were apparent in the ATPi-treated roots (Figure 1D).

Furthermore, we have localized EGO10A-BP in two lines that express the Golgi marker ST-RFP (Teh and Moore, 2007). Despite BFA treatment in the WT (6-1) line, EGO10A-BP and Golgi (ST-RFP) were localized in separate compartments (Figure 1E). However, in the *gnl1-2* line that is flawed in Golgi integrity (Teh and Moore, 2007), EGO10A-BP and ST-RFP were co-localized following BFA treatment to BFA bodies (in addition to the cytoplasmic EGO10A-BP localization). Following, we have localized EGO10A-BP in WT line that expresses endoplasmic reticulum (ER) marker ck-CFP (Nelson et al., 2007). Following BFA treatment and FM46-4 staining, EGO10A-BP signal was detected in the BFA (and cytoplasmic) compartments, but not co-localized with the ER (Figure 1E). Together, these results suggest that following BFA treatment EGO10A-BP is localized to BFA compartments, but not to

the Golgi or ER, and that at least part of EGO10A-BP transport in cells is via a BFA sensitive trafficking system.

Together, the results show that EGO10A-BP is distributed in the roots mainly in the epidermal cell layer. This distribution of EGO10A-BP suggests SLs to be mainly transported in the epidermis cell layer. However it may also derived from the exogenous supplementation of the EGO10A-BP molecule and the plasma-membrane orientation of the transporters in the epidermal cells. Transporters that are localized mostly to the apical plasma membrane in these cells are likely to transport the molecules mostly to apical cells, rather than to those present in adjacent cell layers.

EGO10A-BP molecules are present mostly in the cell cytoplasm. Thus, SLs may be transported symplastically in the plant. Moreover, this transport may be dependent on the structure of the transported molecule, since EGO10B-BP or the EGO10-mD-BP molecules are transported in the root to a lesser extent (Figure 1A). Recently, SL signaling was suggested to take place in the cell nucleus (reviewed by Al-Babili and Bouwmeester, 2015). The activity of EGO10A-BP in terms of root hair elongation suggests that EGO10A-BP penetrated the nuclei at extent sufficient to acknowledge activity.

The high accumulation of EGO10A-BP in cells that were in close contact with the agar cube in the ATPi treatment, and the relatively low level of BP-signal in distant segments of the root in this treatment, suggest that once ATP-dependent processes have been disrupted, SL influx increases and its efflux decreases. Hence, it might be concluded that both the influx and efflux of EGO10A-BP are ATP-dependent, the influx negatively and the efflux positively regulated. Interestingly, auxin influx has been suggested to be gated by an active process that involves plasmodesma-localized callose deposition (Han et al., 2014). The active influx of SLs might rely on a similar gating process. Nevertheless, the absence of a significant difference in shoot-wards vs. root-ward transport of EGO10A-BP in our bioassay suggests a multidirectional flow of SLs. This may be due to the fact that only synthetic analogs were used in the experiments. Also, since EGO10-BP is a synthetic SL analog its transportation within plants may be different from that of natural SLs as the case for auxin analogs. It could also be that our results on the observed regulation of transportation may only be applicable to exogenous SLs but not to endogenous SLs.

The accumulation of SLs in BFA compartments as well as in the cytoplasm suggests that in addition to cytoplasmic diffusion, SLs are secreted via the trafficking system of the cell. Morever, PaPDR1, the Petunia SL transporter, was shown to have a cell-type-specific asymmetric localization in different root tissues, and to be present in the plasma membrane at a polar localizations. Furthermore, treatment with BFA resulted with the accumulation of the GFP-PaPDR1 signal in root cells suggesting that PaPDR1 is trafficked in the cell via a BFA sensitive system (Sasse et al., 2015). Since SL transporters are delivered to the PM by BFA-sensitive trafficking, the presence of SLs in BFA bodies might be a result of this form of trafficking of their transporters. Probable involvement of active SLs trafficking in the cell and the active regulation of SL influx and efflux (see also Kretzschmar et al. 2012; Sasse et al., 2015) suggest that SL transport is a highly regulated process.

Marcelo Fridlender*[1], Beatrice Lace*[2], Smadar Wininger[1], Anandamoy Dam[1], Puja Kumari[1], Eduard Belausov[1], Hanita Tsemach[1], Yoram Kapulnik[1], Cristina Prandi*[2], Hinanit Koltai*[1]

*Equal contribution

[1] Institute of Plant Sciences, Agricultural Research Organization, Volcani Center, Bet Dagan 50250, Israel

[2] Department of Chemistry, University of Turin, via P. Giuria 7 10125 Torino, Italy

References

Al-Babili, S., and Bouwmeester, H.J. (2015). Strigolactones, a Novel Carotenoid-Derived Plant Hormone. Annu. Rev. Plant Biol. 66:161-186.

Cho, M., Lee, S.H., and Cho, H.-T. (2007). P-Glycoprotein4 displays auxin efflux transporter–like action in Arabidopsis root hair cells and tobacco cells. Plant Cell 19:3930-3943.

Cohen, M., Prandi, C., Occhiato, E.G., Tabasso, S., Wininger, S., Resnick, N., Steinberger, Y., Koltai, H., and Kapulnik, Y. (2013). Structure-function relations of strigolactone analogs: activity as plant hormones and plant interactions. Mol. Plant 6:141-152.

Han, X., Hyun, T.K., Zhang, M., Kumar, R., Koh, E.-j., Kang, B.-H., Lucas, W.J., and Kim, J.-Y. (2014). Auxin-callose-mediated plasmodesmal gating is

essential for tropic auxin gradient formation and signaling. Dev. Cell 28:132-146.

Kretzschmar, T., Kohlen, W., Sasse, J., Borghi, L., Schlegel, M., Bachelier, J.B., Reinhardt, D., Bours, R., Bouwmeester, H.J., and Martinoia, E. (2012). A petunia ABC protein controls strigolactone-dependent symbiotic signalling and branching. Nature 483:341-344.

Nelson, B.K., Cai, X., and Nebenführ, A. (2007). A multicolored set of in vivo organelle markers for co-localization studies in Arabidopsis and other plants. Plant J. 51:1126-1136.

Prandi, C., Ghigo, G., Occhiato, E.G., Scarpi, D., Begliomini, S., Lace, B., Alberto, G., Artuso, E., and Blangetti, M. (2014). Tailoring fluorescent strigolactones for in vivo investigations: a computational and experimental study. Org. Biomol. Chem. 12:2960-2968.

Robinson, D. G., Langhans, M., Saint-Jore-Dupas, C., Hawes, C. (2008). BFA effects are tissue and not just plant specific. Trends Plant Sci. 13:405-8.

Sasse, J., Simon, S., Gübeli, C., Liu, G.-W., Cheng, X., Friml, J., Bouwmeester, H., Martinoia, E., and Borghi, L. (2015). Asymmetric Localizations of the ABC Transporter PaPDR1 Trace Paths of Directional Strigolactone Transport. Curr. Biol. 25:647-655.

Teh, O.-k., and Moore, I. (2007). An ARF-GEF acting at the Golgi and in selective endocytosis in polarized plant cells. Nature 448:493-496.

Figure legends

Figure 1. (A) Signal intensity (arbitrary units) of roots treated with EGO10A-BP, EGO10B-BP or EGO10-mD-BP, with and without Antimycin A (ATPi; 10 µM). Signal was quantified (using IMAGEJ) in 9 shoot-ward segments (100 µm each) from the agar cube used to apply the fluorescent molecules to the root. All experiments were repeated at least three times, two replicates per repeat, a minimum of five seedlings per replicate in each experiment. Means of replicates were subjected to statistical analysis by Student's t-test ($P \leq 0.05$). * – Statistically significant differences between means of EGO10A-BP (blue) and EGO10B-BP (light blue) or EGO10-mD-BP (green) treatments. ∓ – Statistically significant differences between means of EGO10A-BP and EGO10A-BP + ATPi treatments. # – Statistically significant differences between means of EGO10-mD-BP and EGO10-mD-BP + ATPi treatments. (B) Root-hair length (µm) in root segments above the agar cubes containing EGO10A-BP, EGO10B-BP, EGO10-mD-BP or naked-BP. All experiments were repeated at least three times, two replicates per repeat, a minimum

of five seedlings per replicate in each experiment. Means of replicates were subjected to statistical analysis by multiple comparison Tukey–Kramer test ($P \leq 0.05$). Different letters above the bars indicate statistically significant differences between means. (C) Images of roots treated with EGO10A-BP or naked-BP. Green- EGO10A-BP or Naked-BP signal, Blue staining- DAPI. Yellow arrows denote the epidermis cell layer. Blue, red and white arrows indicate EGO10A-BP staining in endosomes like bodies, cytoplasm and nucleus envelop, respectively. (D) Images of roots treated with EGO10A-BP or EGO10A-BP + ATPi followed by brefeldin A (BFA). Red – FM4-64 staining; green – EGO10A-BP signal. BFA compartments are indicated by white arrows. Yellow arrows mark EGO10A-BP signal in the cytoplasm. Insert: enlarged BFA body. (E) Images of roots treated with EGO10A-BP followed by brefeldin A (BFA) treatment. In the Golgi marker-expressing lines (WT [6-1] and *gnl1-2*) ST-RFP red – ST-RFP signal; in the endoplasmic reticulum-marker expressing line ER-ck-CFP (CS16256) red – FM4-64 staining; green – EGO10A-BP signal; blue –ER-ck signal. BFA compartments are indicated by white arrows.

Supplemental Figure 1. The molecules used in the present study. The strigolactone (SL) analog EGO10-BP has a SL analog structure functionalized with green BODIPY (BP) as the fluorophore. EGO10A-BP and EGO10B-BP are pure enantiomers which were separated by chiral HPLC. EGO10-mD-BP's structure is the same as the active BODIPY-tagged SL analog EGO10-BP but lacks the D-ring and the enol ether bridge (i.e., bioactiphores). Naked-BP – the BODIPY fluorophore alone.

Supplemental Figure 2. The experimental system. (A) An example of seedlings on plates that were treated with agar cubes containing EGO10A-BP, EGO10B-BP, EGO10-mD-BP or naked-BP. (B) An example of root segments used for quantification of signal intensity in treated roots, shoot-ward or root-ward from the agar cube.

Supplemental Figure 3. (A) Signal intensity (arbitrary units) in roots treated with EGO10A-BP, EGO10B-BP, EGO10-mD-BP or naked-BP. Signal was quantified (using IMAGEJ) in the first shoot-ward or root-ward segment (100 µm) from the agar

cube used to apply the fluorescent molecules to the root. (B) Signal intensity (arbitrary units) of roots treated with EGO10A-BP. Signal was quantified (using IMAGEJ) in 10 shoot-ward or root-ward segments (100 µm each) from the agar cube used to apply the fluorescent molecules to the root. All experiments were repeated at least three times, two replicates per repeat, a minimum of five seedlings per replicate in each experiment. Means of replicates were subjected to statistical analysis by multiple comparison Tukey–Kramer test ($P \leq 0.05$). Lowercase or capital letters above the bars indicate statistically significant differences between means.

Supplemental Figure 4. Root-hair length (µm) in root segments above the agar cubes only (not containing SL analogs) or containing EGO10A, EGO10B, or EGO10-mD, and non-treated control. Experiment consisted of four replicates per repeat, a minimum of ten seedlings per replicate. Means of replicates were subjected to statistical analysis by multiple comparison Tukey–Kramer test ($P \leq 0.05$). Different letters above the bars indicate statistically significant differences between means.

Supplemental Figure 5. Examples to images of roots treated with EGO10A-BP. Green- EGO10A-BP signal, Blue staining- DAPI. White arrows denote EGO10A-BP staining in nucleus.

Supplemental Figure 6. (A) EGO10A-BP signal in root segments that were covered with agar cubes containing EGO10A-BP or EGO10A-BP + Antimycin A (ATPi). Roots were uncut and agar cube was removed to reveal the part of the root below it. (B) Images of roots treated with EGO10A-BP and ATPi. Green - EGO10A-BP; blue - DAPI staining.

Supplemental Figure 7. Linear-regression formula of graph of signal intensity (arbitrary units) in roots treated with EGO10A-BP or EGO10A-BP + Antimycin A (ATPi). Signal was quantified (using IMAGEJ) in the first three shoot-ward segments (100 µm each) from the agar cube used to apply the fluorescent molecules to the root. All experiments were repeated at least three times, two replicates per repeat, a minimum of five seedlings per replicate in each experiment. Means of replicates were

subjected to statistical analysis by multiple comparison Tukey–Kramer test ($P \leq 0.05$). Capital letters indicate statistically significant differences between means.

Supplemental Figure 8. EGO10-BP synthetic pathway, which gives as products a racemic mixture of two enantiomers. For EGO10-mD-BP the amino intermediate 5 is coupled with the BODIPY activated ester 10 without performing the attachment of the D-ring.

Supplemental Figure 9. 1H and 13C NMR spectra of EGO10-mD-BP

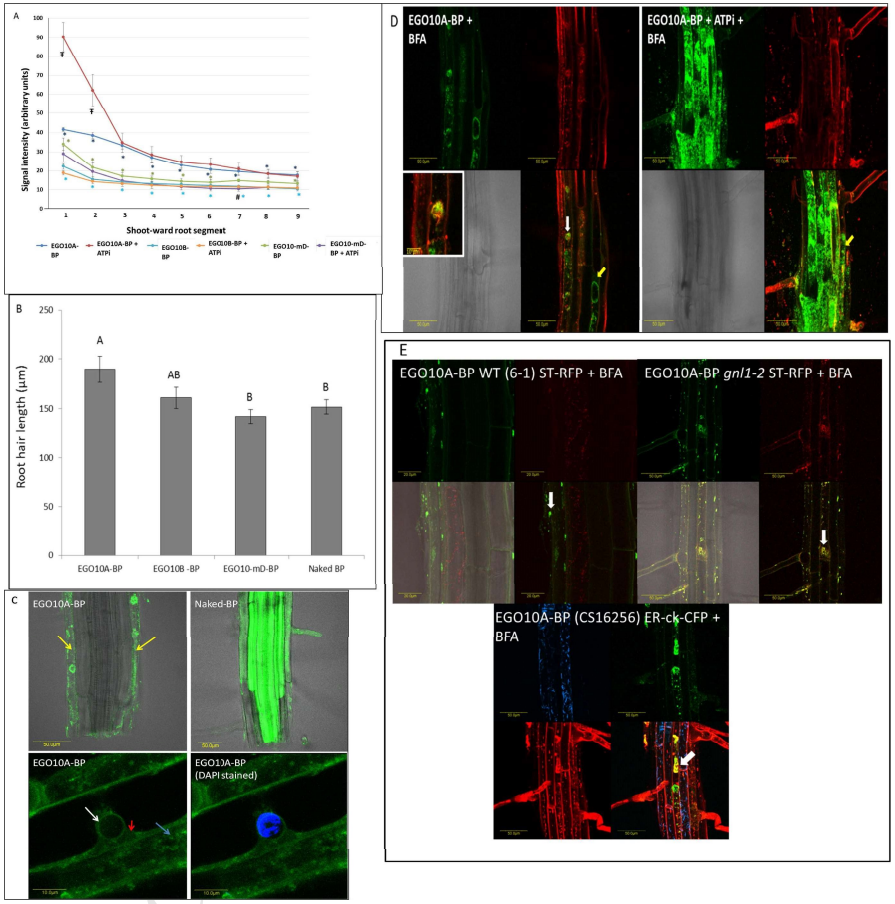

Figure 1. (A) Signal intensity (arbitrary units) of roots treated with EGO10A-BP, EGO10B-BP or EGO10-mD-BP, with and without Antimycin A (ATPi; antimycin A, 10 µM). Signal was quantified (using IMAGEJ) in 10 shoot-ward segments (100 µm each) from the agar cube used to apply the fluorescent molecules to the root. All experiments were repeated at least three times, two replicates per repeat, a minimum of five seedlings per replicate in each experiment. Means of replicates were subjected to statistical analysis by Student's t-test ($P \leq 0.05$). * – Statistically significant differences between means of EGO10A-BP (blue) and EGO10B-BP (light blue) or EGO10-mD-BP (green) treatments. ∓ – Statistically significant differences between means of EGO10A-BP and EGO10A-BP + ATPi treatments. # – Statistically significant differences between means of EGO10-mD-BP and EGO10-mD-BP + ATPi treatments. (B) Root-hair length (µm) in root segments above the agar cubes containing EGO10A-BP, EGO10B-BP, EGO10-mD-BP or naked-BP. All experiments were repeated at least three times, two replicates per repeat, a minimum of five seedlings per replicate in each experiment. Means of replicates were subjected to statistical analysis by multiple comparison Tukey–Kramer test ($P \leq 0.05$). Different letters above the bars indicate statistically significant differences between means. (C) Images of roots treated with EGO10A-BP or naked-BP. Green- EGO10A-BP or Naked-BP signal, Blue staining- DAPI. Yellow arrows denote the epidermis cell layer. Blue, red and white arrows indicate EGO10A-BP staining in endosomes like bodies, cytoplasm and nucleus envelop, respectively. (D) Images of roots treated with EGO10A-BP or EGO10A-BP + ATPi followed by brefeldin A (BFA). Red – FM4-64 staining; green – EGO10A-BP signal. BFA compartments are indicated by white arrows. Yellow arrows mark EGO10A-BP signal in the cytoplasm. Insert: enlarged BFA body. (E) Images

of roots treated with EGO10A-BP followed by brefeldin A (BFA) treatment. In the Golgi marker-expressing lines (WT [6-1] and *gnl1-2*) ST-RFP red – ST-RFP signal; in the endoplasmic reticulum-marker expressing line ER-ck-CFP (CS16256) red – FM4-64 staining; green – EGO10A-BP signal; blue –ER-ck signal. BFA compartments are indicated by white arrows.